Monthly Notices
of the
ROYAL ASTRONOMICAL SOCIETY

Mon. Not. R. Astron. Soc. **423,** 3243–3250 (2012) doi:10.1111/j.1365-2966.2012.21113.x

Effects of baryon mass loss on profiles of large galactic dark matter haloes

Cinthia Ragone-Figueroa,[1⋆] Gian Luigi Granato[2⋆] and Mario G. Abadi[1⋆]

[1]*Instituto de Astronomía Teórica y Experimental, IATE, CONICET-Observatorio Astronómico, Universidad Nacional de Córdoba, Laprida 854, X5000BGR Córdoba, Argentina*
[2]*Istituto Nazionale di Astrofisica INAF, Osservatorio Astronomico di Trieste, Via Tiepolo 11, I-34131 Trieste, Italy*

Accepted 2012 April 14. Received 2012 March 26; in original form 2012 January 30

ABSTRACT

We perform controlled numerical experiments to asses the effect of baryon mass loss on the inner structure of large galactic dark matter (DM) haloes. This mass expulsion is intended to mimic both the supernova and active galactic nucleus (AGN) feedbacks, as well as the evolution of stellar populations. This study is meant in particular for precursors of massive early-type galaxies (ETGs), wherein strong AGN feedback (often dubbed 'quasi-stellar object mode' in galaxy formation models) has been proposed to remove on a short time-scale, of the order of a few dynamical times, a substantial fraction of their baryons. In a previous paper we evaluated the observational consequences (size increase) of this process on the galactic structure. Here we focus on the distribution of DM in the galactic region. It is shown that the inner region of the DM halo expands and its density profile flattens by a sizeable amount, with little dependence on the expulsion time-scale. We also evaluate the effect of the commonly made approximation of treating the baryonic component as a potential that changes in intensity without any variation in shape. This approximation leads to some underestimates of the halo expansion and its slope flattening. We conclude that cuspy density profiles in ETGs could be difficult to reconcile with an effective AGN (or stellar) feedback during the evolution of these systems.

Key words: methods: numerical – galaxies: elliptical and lenticular, cD – galaxies: evolution – galaxies: formation – galaxies: haloes – quasars: general.

1 INTRODUCTION

A long-standing puzzle of post-recombination cosmology based on cold dark matter (CDM), independently of the presence of cosmological constant or curvature in the adopted cosmological model, is the so-called *core–cusp* problem (for a recent review, see De Blok 2010). Since the 1990s, a long series of *N*-body (gravity-only) simulations, dating back to Dubinski & Carlberg (1991), has produced dark matter haloes (DMHs) whose inner density profile is reasonably well described by a power law $\rho \propto r^{\alpha}$, with $\alpha \sim -1$, i.e. a cusp. This is at odds with several observations, suggesting a flat density profiles of DM in the inner region of real galaxies, i.e. a core. The case for cored DM density profiles is rather strong in dwarf galaxies and disc-dominated low surface brightness (LSB) galaxies, wherein the dynamics of visible matter tracks safely the largely dominating gravitational field of DM. Also, the dynamics of normal spiral galaxies is best interpreted by means of cored DM mass models (e.g. Salucci & Frigerio Martins 2009, and references therein), while the presence of a core in DMHs of large elliptical galaxies is difficult to assess and controversial (e.g. Memola, Salucci & Babić 2011; Sonnenfeld et al. 2011; Tortora et al. 2012), since their central region is even more gravitationally dominated by the baryon component, and because the orbital structure cannot be interpreted straightforwardly.

A widespread idea is that the solution to the core–cusp problem should be searched for in the physics of baryonic matter, which can affect to some extent the distribution of DM in the inner region of haloes, and is not included in the aforementioned computations.

However, the first baryonic process expected to occur worsens the problem. It consists in some further contraction of the central region of the DMH, induced by the much stronger concentration collapse of dissipative baryonic matter (e.g. Blumenthal et al. 1986; Gnedin et al. 2004; Abadi et al. 2010; Gnedin et al. 2011). The exact importance of this process is somewhat debated. Different numerical works found different results and significantly less contraction than that predicted by the simple analytic estimate by Blumenthal et al. (1986). In any case, this mechanism produces some further steepening of the inner profile, with respect to the prediction of gravity-only cosmological simulations.

⋆E-mail: cin@oac.uncor.edu (CR-F); granato@oats.inaf.it (GLG); mario@oac.uncor.edu (MGA)

Nevertheless, several subsequent (and more complex) baryon processes occur after this primary condensation and can act in the opposite direction. Indeed, they have been often evaluated specifically to seek solutions to the core–cusp problem (e.g. Navarro, Eke & Frenk 1996; Gnedin & Zhao 2002; Read & Gilmore 2005; Mashchenko, Couchman & Wadsley 2006; Tonini, Lapi & Salucci 2006; Mashchenko, Wadsley & Couchman 2008; Governato et al. 2010; Pasetto et al. 2010; De Souza et al. 2011; Inoue & Saitoh 2011; Martizzi et al. 2012; Ogiya & Mori 2011; Macciò et al. 2012; Pontzen & Governato 2012). Several of these papers have addressed the effect of baryon ejection, due to supernova (SN) feedback, on the central DM density profile of less massive systems, i.e. mainly dwarfs or at most disc-dominated galaxies. The results on its importance have been sometimes contradictory (for a discussion of possible causes, see Read & Gilmore 2005).

Much less attention has been paid so far to these effects in larger systems, such as early-type galaxies (ETGs). The main reason is obviously that their DM content is less constrained by the data, as noted above (see Buote & Humphrey 2012, for a review). Moreover, mechanisms related to SN feedback are expected to be less effective in the deeper potential wells of large ETGs. As for the first point, it is worth noting that recent observational evidence points to a DM distribution either shallower (Memola et al. 2011) or cuspier (Sonnenfeld et al. 2011; Tortora et al. 2012) than that predicted by ΛCDM gravity-only simulations. New techniques could soon provide constrains on the DM distribution in ellipticals (e.g. Pooley et al. 2012). As for the second point, in the past few years it has become common to consider in galaxy formation theory the feedback of active galactic nucleus (AGN) activity, which is likely to be much more effective in massive systems than that due to SNe (e.g. Silk & Rees 1998; Fabian 1999; Granato et al. 2001, 2004; Benson et al. 2003; Cattaneo et al. 2006; Monaco, Fontanot & Taffoni 2007; Sijacki et al. 2007; Somerville et al. 2008; Ciotti, Ostriker & Proga 2009; Johansson, Naab & Burkert 2009). AGN feedback is widely considered the most promising mechanism for relaxing those tensions between galaxy formation models and observation, broadly related to the so-called *overcooling problem*. This is the tendency of models to produce too massive and too blue (i.e. star-forming) galaxies at low redshift, and to lock up in galaxies an excessive fraction of available baryons. On the contrary, many observations indicate that on average the more massive a galaxy is, the earlier it stops its star formation activity, a phenomenon referred to as *downsizing* (e.g. Brammer et al. 2011; for a critical discussion of the various manifestations of downsizing, see Fontanot et al. 2009). Despite the likely prominent role of AGN feedback in galaxy formation, so far its effect on the DM distribution has not been evaluated in detail (but see Peirani, Kay & Silk 2008; Duffy et al. 2010).

One kind of AGN feedback [that is sometimes called 'quasi-stellar object (QSO) mode'] is expected to eject on a small timescale (of the order of a few $\times 10$ Myr at most) the cold gas not yet converted into stars in star-forming ETGs. In a recent work (Ragone-Figueroa & Granato 2011, henceforth Paper I), we have evaluated with aimed numerical simulations the importance of this process, concentrating our analysis on the baryon component of ETGs, in order to asses its possible contribution to the observed size evolution of ETGs (see e.g. Newman et al. 2012, and references therein). In this paper we investigate instead in detail the effects on the profile of the DMH.

Since we are mainly interested in ETGs rather than less massive systems such as dwarfs, we will extend the studies already published to regions of the parameter space not covered previously. Indeed, this is the first work where the initial conditions (ICs) have been thought to get a configuration, after the loss of a substantial fraction of baryons previously condensed in the central region of the DMH (i.e. the galactic region), consistent with our basic knowledge of the properties of local large ETGs (baryon-to-DM mass ratio, scalelengths and size as a function of stellar mass). By converse, in most studies the baryons totally disappear, or the remaining fraction is $\leq$5 per cent, consistently with the very low baryon content of dwarf galaxies. This is not the case for ETGs, where the leftover baryons still dominate the potential wells in the central region of the DMH. Also, in order to asses the maximal effect of baryon loss, in most studies the initial mass ratio of condensed baryon to DM has been set close to the cosmic baryon fraction. However, this appears too extreme, at least for ETGs. According to the cooling prescriptions adopted by semi-analytic models and simulations of galaxy formation, no more than a few tens of per cent of the cosmic baryons had time to cool and condense in a large galactic DMH during the few Gyr over which ETGs formed at $z \gtrsim 1.5$ (e.g. Benson et al. 2001; Helly et al. 2003; Granato et al. 2004; Cattaneo et al. 2007; Viola et al. 2008). We point out explicitly that the results of previous numerical experiments, when featuring substantial differences in the initial and/or final mass ratios of baryon to DM, or in the assumed density profiles of the two components (often discs for the baryons), cannot be simply rescaled to predict quantitatively our findings.

Moreover, a technical difference with respect to most previous similar works is that often the baryon component has been treated as a fixed shape (rigid) potential. Here in general we do not adopt this approximation (since in Paper I we wanted to actually study the expansion of leftover baryons), but we evaluate its effect.

The organization of the paper is straightforward: in Section 2 we describe the ICs and method for our simulations, whose result are presented in Section 3. The implications for our understanding of ETG formation are discussed in Section 4.

2 NUMERICAL METHOD AND SETUP

The setup of the simulations used in this paper is similar to that described in Paper I, to which we refer for a few more details. The main difference is that here we also run simulations in which the ICs take into account the possible halo contraction due to baryon condensation. Moreover, we evaluated the effect of the approximation of treating the baryons as a fixed shape potential.

The purpose of the simulations is to investigate the evolution of collisionless particles (stars and DM) under a change of gravitational potential due to a loss of baryonic mass of the system. In general, the escaping mass can represent either the gas which has not been converted into stars during the star-forming phase of the spheroid (ejected by feedback driven galactic winds) or the mass lost from stars in the form of stellar winds and SN explosions (which is likely to escape the ETG potential wells). In any case, we assume as given, and due to causes not included in our physical treatment (such as SN and AGN feedbacks or stellar evolution), the temporal dependence of this mass loss (equation 10), which we put by hand, and we simulate the ensuing dynamical evolution of collisionless mass distributions. Therefore we do not have to treat the gas dynamics.

We used the public version of the code GADGET-2 (Springel 2005) to perform simulations with 10^6 and 5×10^6 particles in the gravity-only mode. None of the presented results shows any noticeable difference in the two cases, which assures us that the mass resolution is sufficient for the purposes of the present study. Half of the particles are used to sample the baryonic and dark matter components with a

softening of 0.007 and 0.35 kpc, respectively. We checked that our results are not affected by significant variations in these choices.

The density distribution of DM particles is initially (i.e. even before computing the effects of baryonic contraction; see below) assumed to follow the standard NFW (Navarro, Frenk & White 1997) shape:

$$\rho_{\rm DM}(r) = \frac{M_{\rm vir,DM}}{4\pi\, R_{\rm vir}^3}\, \frac{c^2\, g(c)}{\hat{r}\,(1+c\,\hat{r})^2}, \tag{1}$$

where $M_{\rm vir,DM}$ is the halo virial mass in DM (the DM mass inside $R_{\rm vir}$), $\hat{r} = r/R_{\rm vir}$, c is the concentration parameter and $g(c) \equiv [\ln(1+c) - c/(1+c)]^{-1}$.

The virial radius $R_{\rm vir}$ is by definition the radius within which the mean density is $\Delta_{\rm vir}(z_{\rm vir})$ times the mean matter density of the Universe $\rho_{\rm u}(z_{\rm vir})$ at virialization redshift $z_{\rm vir}$:

$$R_{\rm vir} = \left[\frac{3}{4\pi}\, \frac{M_{\rm vir}}{\Delta_{\rm vir}(z_{\rm vir})\rho_{\rm u}(z_{\rm vir})}\right]^{1/3}. \tag{2}$$

The overdensity $\Delta_{\rm vir}(z)$, for a flat cosmology, can be approximated by

$$\Delta_{\rm vir}(z) \simeq \frac{(18\pi^2 + 82x - 39x^2)}{\Omega(z)}, \tag{3}$$

where $x = \Omega(z) - 1$ and $\Omega(z)$ is the ratio of the mean matter density to the critical density at redshift z (Bryan & Norman 1998). The corresponding mass distribution is written as

$$M_{\rm DM}(<r) = M_{\rm vir,DM}\, g(c)\, \left[\ln(1+c\,\hat{r}) - \frac{c\,\hat{r}}{(1+c\,\hat{r})}\right]. \tag{4}$$

For the collisionless baryonic particles (representing the potential of both stars as well as gas before expulsion), we assume that, as a result of the assembly of the central galaxy, they settle on an Hernquist (1990) profile, which provides a reasonable description of stellar density in spheroids:

$$\rho_{\rm B}(r) = \frac{M_{\rm B}}{2\pi}\, \frac{a}{r}\, \frac{1}{(r+a)^3}, \tag{5}$$

where $M_{\rm B}$ is the total baryonic mass. The corresponding mass distribution is

$$M_{\rm B}(<r) = M_{\rm B}\, \left(\frac{r}{r+a}\right)^2, \tag{6}$$

so that the half-mass radius is related to the scale radius a by $R_{1/2} = (1+\sqrt{2})\, a$ and, assuming a mass-to-light ratio independent of r, the effective radius is $R_{\rm e} \simeq 1.81a$.

As discussed in Section 1, the process of baryon condensation in the centre of the DMHs is expected to contract to some extent the DM distribution. Since, at variance with Paper I, the target of this study is precisely to evaluate the effect of baryon expulsion on DMH density profiles, we also performed runs including an estimate of the contraction in the ICs by adopting the Abadi et al. (2010) prescriptions. They found that a simple formula captures the average behaviour of their simulations:

$$r_{\rm f}/r_{\rm i} = 1 + \alpha\, \left[(M_{\rm i}/M_{\rm f})^n - 1\right], \tag{7}$$

where n and α are parameters (see below). This equation relates the initial (i.e. before baryon condensation) and final radii of the spheres containing the same amount of DM to the *total* masses $M_{\rm f}$ and $M_{\rm i}$ within the same spheres. Since

$$\frac{M_{\rm f}}{M_{\rm i}} = \frac{M_{\rm f,DM}(<r_{\rm f}) + M_{\rm f,bar}(<r_{\rm f})}{M_{\rm i,DM}(<r_{\rm i}) + M_{\rm i,bar}(<r_{\rm i})}, \tag{8}$$

where $M_{\rm f,DM}(<r_{\rm f}) = M_{\rm i,DM}(<r_{\rm i})$, by definition of $r_{\rm i}$ and $r_{\rm f}$, once it is assumed an initial density distribution for DM and baryons and a final density distribution for baryons, equation (7) is an implicit equation for $r_{\rm f}$ given an $r_{\rm i}$, which can be solved numerically to obtain the final mass distribution of DM, $M_{\rm f,DM}(<r)$. As stated by Abadi et al. (2010), their results are well described, setting $n = 2$ and $\alpha = 0.3$. Moreover, the contraction predicted by Blumenthal et al. (1986) as well as that found in simulations by Gnedin et al. (2004) are well described, setting $n = 1$ and $\alpha = 1$ or 0.73, respectively. When exploiting equation (7), we describe the initial mass distribution of DM and the final mass distribution of baryons with equations (4) and (6). Also, we assume that before contraction, baryons follow the same density distribution of DM (equation 1); rescaled by the cosmic baryon fraction we assume $f_{\rm b} = \Omega_{\rm bar}/\Omega_{\rm m} = 0.17$ (consistent with cosmic microwave background 7-year *Wilkinson Microwave Anisotropy Probe* constraints; Komatsu et al. 2009).

In the following, unless otherwise specified, by *dynamical time* $t_{\rm dyn}$ we mean the initial (i.e. before any mass loss and expansion) dynamical time, computed at baryon $R_{1/2}$:

$$t_{\rm dyn} = \left[\frac{R_{1/2}^3}{2\,G\,\left(M_{\rm B}/2 + M_{\rm DM}(<R_{1/2})\right)}\right]^{1/2}. \tag{9}$$

Even though in this paper our focus is on the evolution of the DM component of the system, we maintain the same definition of dynamical time as in Paper I, since the effects under study are confined to the inner region of the DM distribution.

Given the density profiles, we obtain the 1D velocity dispersion by integrating the Jeans equation under the assumption of isotropic conditions. To generate the ICs, we randomly populate the system with baryonic and DM particles, according to the density distributions (equations 5 and 1). The particles velocities are randomly generated assuming local Maxwellian distribution with 1D velocity dispersion obtained by the solution of Jeans equation. Then, by numerically evolving the system for several dynamical times, we obtain a (quasi-)static statistical equilibrium. This latter step does not produce significant variations in the density profiles (see discussion of Fig. 1 in Section 3 for more details).

Starting from this initial setup, we introduce a mass loss by removing exponentially during an ejection time interval Δt a fraction $1-\epsilon$ of the baryonic mass:

$$M_{\rm B}(t) = M_{\rm B(}t=0{\rm)}\, \exp\left(\frac{\ln\epsilon}{\Delta t}\, t\right). \tag{10}$$

The mass loss is practically attained by decreasing correspondingly in time the mass of the baryonic particles sampling the density field. After the end of the mass-loss period Δt, we let the system to evolve till it reaches a new equilibrium configuration.

We also wanted to study the effect of a common approximation done when evaluating the evolution of the DM distribution under a baryon mass loss, namely to treat the baryonic component as a potential that changes in intensity without any variation in shape (a rigid potential; e.g. Navarro et al. 1996; Ogiya & Mori 2011). For this purpose, we also run simulations in which the positions of baryonic particles were not updated in time.

The reference value for the initial (i.e. before any mass loss) ratio of virial mass (total mass within the virial radius) to baryonic mass is $M_{\rm vir}/M_{\rm B(}t=0{\rm)} = 20$. This value is in keeping with the 20–40 per cent fraction of cosmic baryons that can cool and condense in the central region of a large galactic DMH at $z \gtrsim 1.5$, according to the prescriptions adopted by semi-analytic models and simulations of galaxy formation (e.g. Benson et al. 2001; Helly et al. 2003;

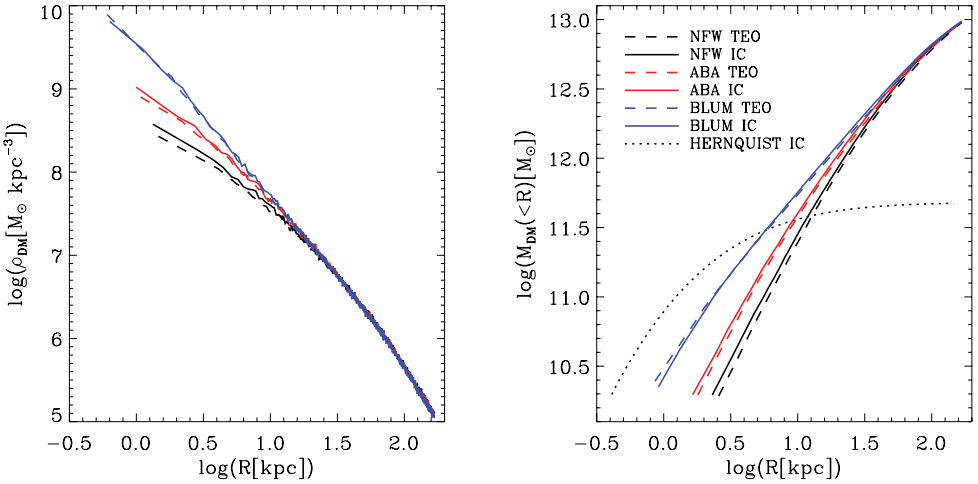

Figure 1. The curve marked NFW TEO represents the typical density run of DMHs produced by gravity-only simulations (Navarro et al. 1997), whilst ABA TEO and BLUM TEO are intended to keep into account the contraction resulting from galaxy formation, as described in Section 2. After setting these theoretical ICs (dashed lines in both panels), we let each system to evolve, for 0.4 Gyr, into an equilibrium configuration. These are considered the ICs for the numerical experiments before forcing baryon mass loss. The density and mass profiles are shown in the left- and right-hand panels, respectively. In addition, we show in the right-hand panel the Hernquist profile mass corresponding to the baryonic component.

Granato et al. 2004; Cattaneo et al. 2007; Viola et al. 2008). Moreover, assuming that after the initial condensation the halo loses, due to feedback-induced galactic winds, a fraction of between 20 and 80 per cent of this 'galactic' baryonic mass, it is left with a baryon to DM content, broadly consistent with estimates in the local Universe for large galactic haloes (Moster et al. 2010).

We set $M_{\rm vir} = 10^{13}\,{\rm M}_{\odot}$ in all simulations. Nevertheless, our results apply to different values of $M_{\rm vir}$, provided that the ratios of scale radii and masses in the two components (DM and baryons) are not changed and the time is measured in units of dynamical time $t_{\rm dyn} \propto \rho^{-1/2}$.

We adopt a concentration parameter $c = 4$, a typical value at galactic halo formation (see Zhao et al. 2003; Klypin, Trujillo-Gomez & Primack 2011), and $R_{\rm vir} \simeq 170\,{\rm kpc}$ [from equations (2) and (3), with $M_{\rm vir} = 10^{13}\,{\rm M}_{\odot}$ and $z_{\rm vir} = 3$].

Finally, we set $a = 1.5\,{\rm kpc}$ ($R_{\rm e} \simeq 2.7\,{\rm kpc}$). We refer the reader to Section 3 of Paper I for motivations for this values. The initial (i.e. before mass loss and expansion, equation 9) dynamical time as defined above is $t_{\rm dyn} \approx 5\,{\rm Myr}$.

In summary, the parameters affecting the results of our simulations are the ratio of mass between the total and baryonic components $M_{\rm vir}/M_{{\rm B}(t\,=0)}$, the corresponding ratio of scalelengths $R_{\rm vir}/a$, the fraction of baryon mass lost $(1 - \epsilon)$ and the time Δt over which the loss occurs. We performed simulations covering broad ranges of the latter two quantities, while in most runs we kept the former two at the fiducial values reported above. We checked, however, that none of our qualitative conclusion is affected by a factor of $\sim$2 variations of them (Paper I and some more discussion in Section 3).

3 RESULTS

Fig. 1 shows the initial equilibrium density and mass profiles for the DM component, i.e. those adopted before forcing any loss of baryonic mass (solid lines). The right-hand panel also displays the adopted standard Hernquist mass profile for the baryons. Here and in the following, the lower limit of the density and mass profile plots equals the adopted gravitational softening for the DM component, and the density and the accumulated mass are evaluated using radial bins containing $\simeq$500 DM particles. These initial profiles are obtained letting to evolve for several tens of dynamical times the composite system, where for the DM component we adopted the pure NFW mass profile (black dashed line), or the profiles implicitly given by equation (7), with values of the n and α parameters adequate to reproduce the contraction found by Abadi et al. (2010) in simulations (red dashed line) or that analytically predicted by Blumenthal et al. (1986) (blue dashed line), as detailed in Section 2. We refer to these three cases as NFW, ABA and BLUM, respectively. The first and the last should be regarded as extreme cases where the effect of contraction is negligible and maximal, respectively, while the intermediate case, ABA, is likely to be more realistic. The numerical evolution does not affect much the initial configuration of DM. For instance, the local power-law index of the density distribution increases in the inner $\sim$10 kpc by less than 0.1, making it slightly steeper. The effect decreases with increasing contraction of the DM profiles, i.e. from NFW to BLUM. Kazantzidis, Magorrian & Moore (2004) suggested that the local Maxwellian assumption employed here (and in many other works) to set up the ICs can lead to spurious results in the study of long-term evolution of DMHs. In particular, they found that the central cusp is quickly significantly reduced. In our case, we find a much less important, and opposite, trend. We attribute this to the presence of the dominating baryonic component in the centre of the halo, not included in the study by Kazantzidis et al. (2004). Indeed, on the one hand, we run a pure DM test case, which confirmed their result on the reduction of the central cusp. On the other hand, we note that Read & Gilmore (2005), who considered composite baryon plus DM systems as we did, also found excellent agreement between ICs generated with the Maxwellian approximation and with the alternative procedure proposed by Kazantzidis et al. (2004).

In addition to the three cases NFW, ABA and BLUM, and in order to study the dependence of our results on the parameters of the initial baryonic configuration, we considered ICs in which we halved the scale radius of the baryonic component (henceforth ABA HALFSIZE) or we doubled its mass. We then correspondingly contract the DMH as we did for ABA. The direction of these variations

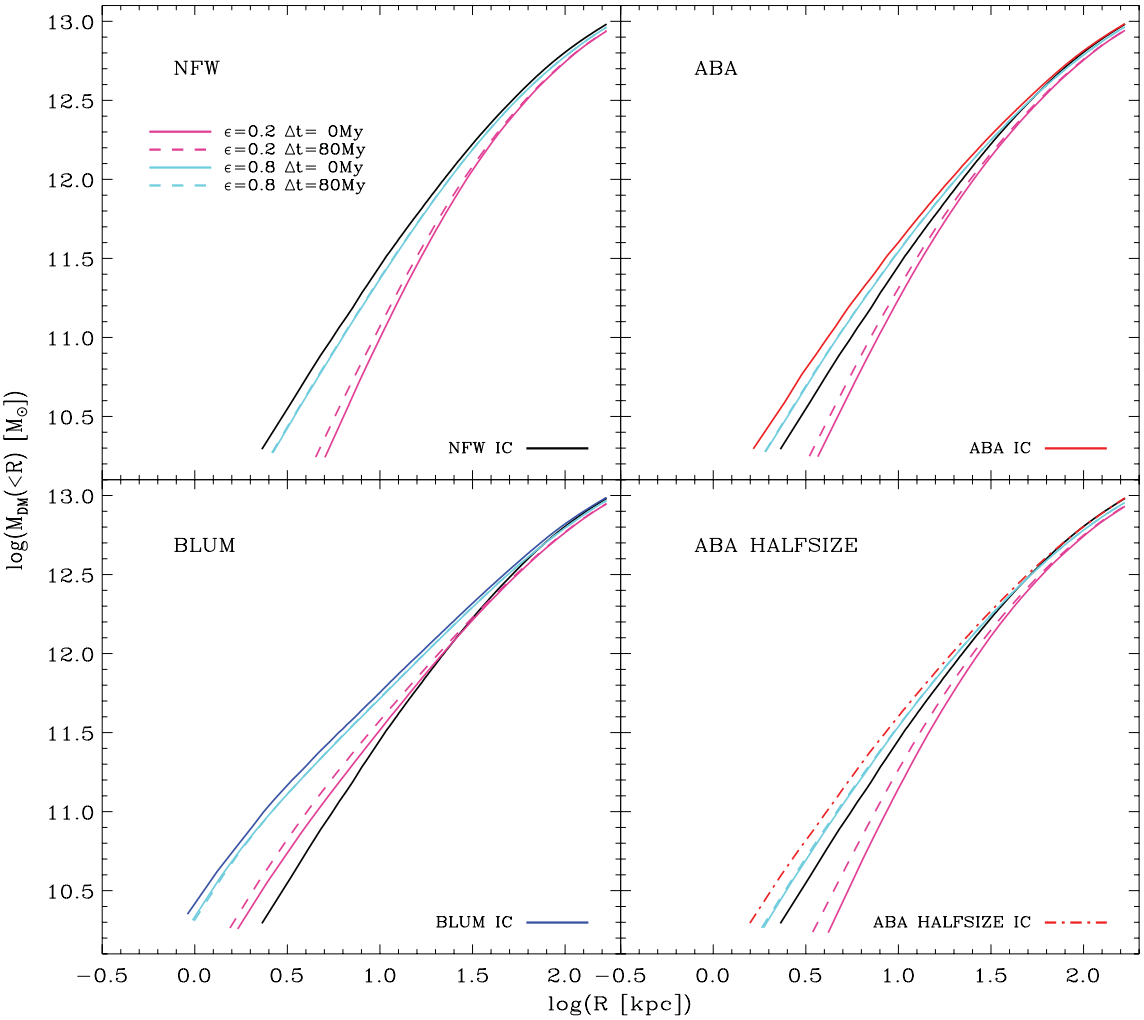

Figure 2. Comparison between the initial and final mass profiles. The latter is the new equilibrium configuration reached ∼0.2 Gyr after the baryonic mass loss (see Fig. 4). Each panel refers to simulations performed adopting a different initial density profile, as indicated by the inner label, which is plotted with the same colour as in the previous figure. ABA HALFSIZE IC (bottom-right panel) is obtained as ABA IC, but halving the Hernquist scale radius of the baryonic component. The final profiles for $\epsilon = 0.2$ and 0.8 are in magenta and cyan, respectively; solid lines are for $\Delta t = 0$ Myr (instantaneous baryon expulsion) and dashed lines for $\Delta t = 80$ Myr (barely distinguishable for the lower mass loss $\epsilon = 0.8$). In all the panels, we also plot for reference the standard NFW profile (black solid line).

has been elected in order to increase the effect of mass loss with respect to the standard case. These two ICs are not shown in Fig. 1, since they are almost indistinguishable from the ABA IC.

Figs 2 and 3 display the effect of baryon mass loss on the initial mass distributions described above. The four panels in each figure correspond to the ICs dubbed NFW, ABA, BLUM and ABA HALFSIZE. The new equilibrium configurations, shown in the figures, are reached typically a few tens of dynamical times (equation 9) after the end of the mass-loss period (Δt), as can be appreciated in Fig. 4. Whenever the fraction of baryon mass loss is important (say $\gtrsim$50 per cent), the final DM profile is significantly flatter in the centre than the initial one. If this is the case, the ensuing expansion more than counteracts the opposite contraction caused by baryon condensation, at least that found in recent numerical simulations (Abadi et al. 2010) (see the right-hand panels). The effect is somewhat weaker when the DM profile is initially more concentrated, as expected, since in this case the contribution of DM to the gravitational field in the centre becomes more important. For the same reason, the flattening effect in ABA HALFSIZE is slightly enhanced with respect to ABA. Indeed, in the former ICs, the contribution to the initial equilibrium of the baryons that we let to escape during mass loss was higher. To a lesser extent, the same happens doubling the initial baryon mass, but the difference is barely visible, so that we do not plot this case.

The dependence on the time-scale of the mass loss is weak. This finding is at variance with respect to the result by Ogiya & Mori (2011), who found that if the loss is slow enough, the DM profiles are much less affected, up to the point that after a while it returns very close to the ICs. We have checked that this result is not due to the approximation used by Ogiya & Mori of treating the baryons as a fixed form potential (see below). This difference could arise in part, but not entirely, from the more compact baryon distribution adopted by these authors. Actually, we find a somewhat more evident dependence on time-scale when the baryon component is initially more concentrated (ABA HALFSIZE; lower-right panels). It is also interesting to note that the expansion of the baryonic

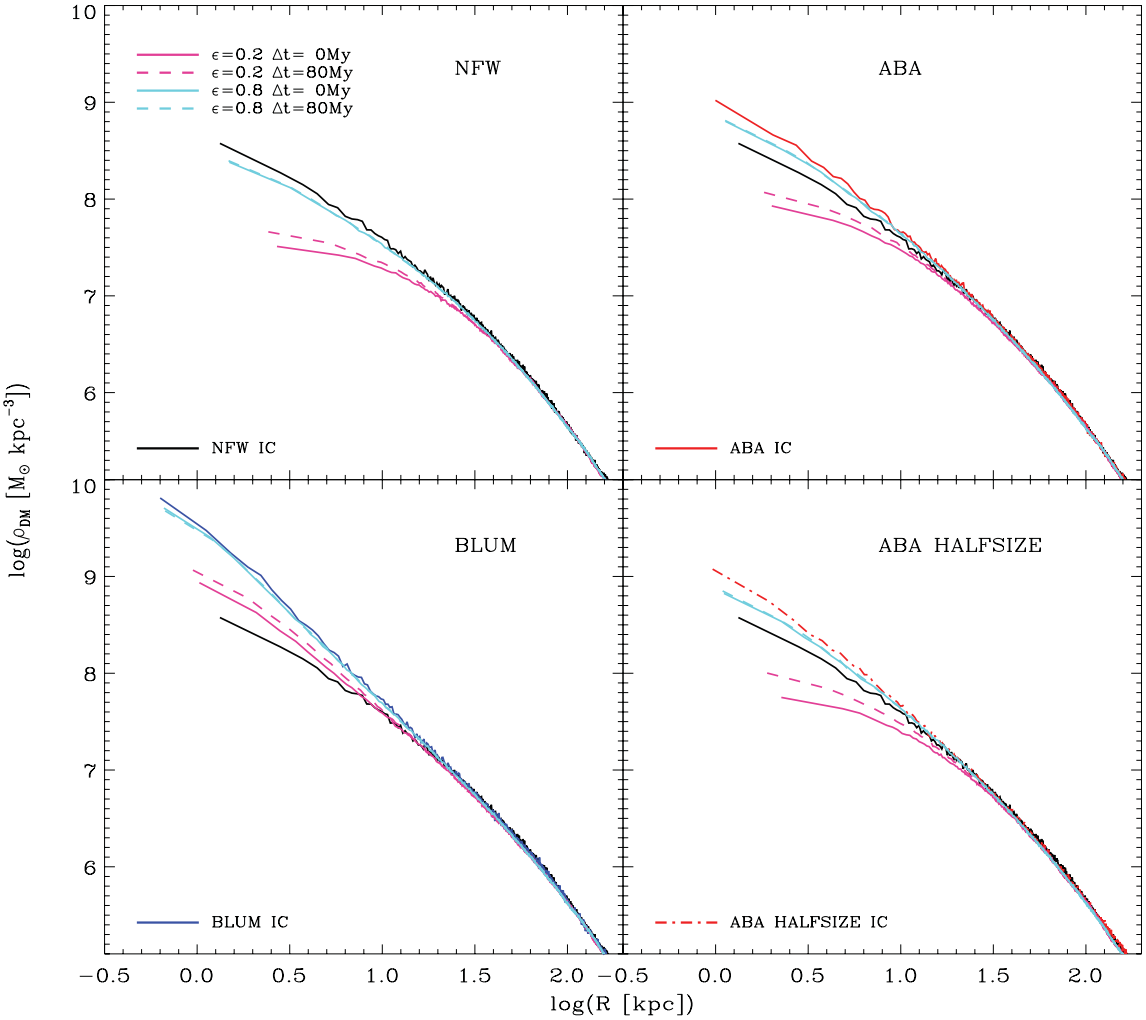

Figure 3. The same as the previous figure but comparing the initial and final density profiles. The different panels correspond to different ICs as labelled in the plot.

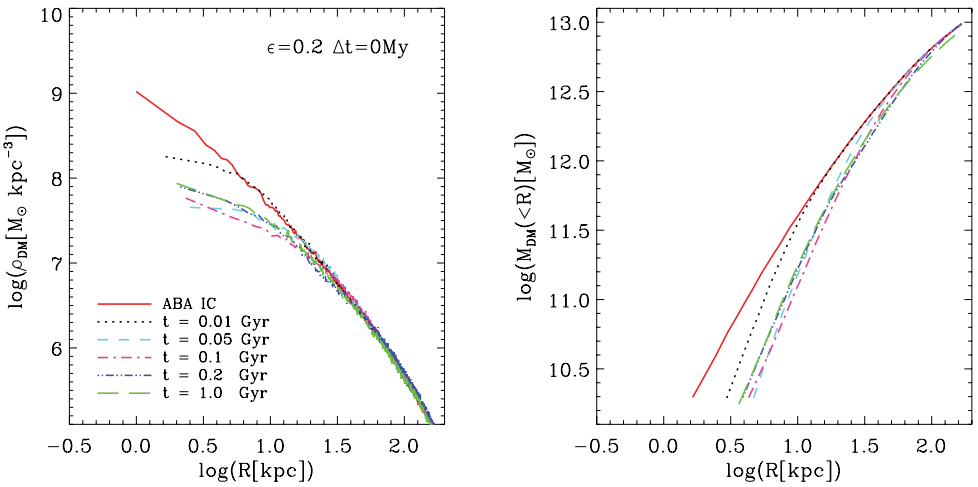

Figure 4. Time evolution, after the baryon mass loss of the density (left-hand panel) and mass (right-hand panel) DM profiles for one of our simulations, namely the case ABA with instantaneous mass loss $\Delta t = 0$ Gyr and $\epsilon = 0.2$. The new equilibrium is reached within ∼0.2 Gyr, i.e. within 40 dynamical times of the central region (equation 9). This holds true for all the other cases.

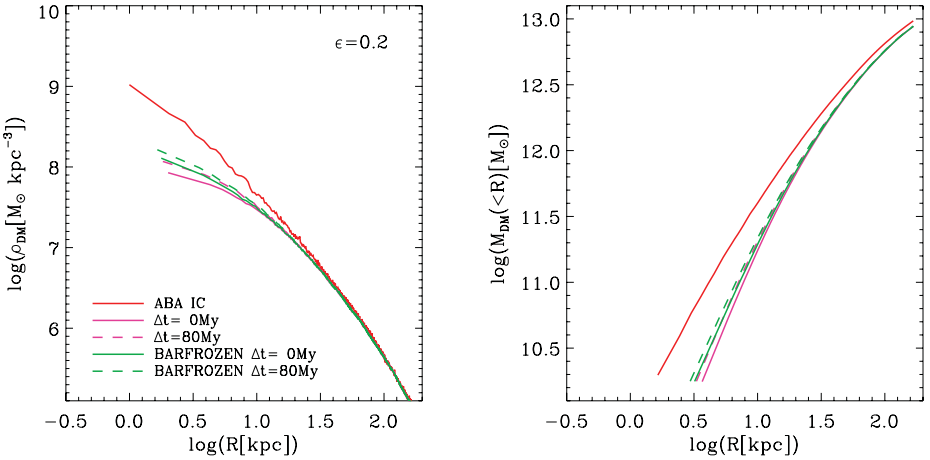

Figure 5. Comparison between the new equilibrium DM density (left-hand panel) and mass (right-hand panel) profiles after baryon mass loss, for $\epsilon = 0.2$, obtained letting the baryon particles to adjust their position according to the change of potential (magenta lines), or keeping their position fixed (green lines). The former is the treatment adopted in this work, while the latter corresponds to the common approximation of treating the baryons as a rigid potential.

mass distribution is much more affected than that of the DM by the time-scale of expulsion (see Paper I for details).

In Fig. 4 we show the time evolution of the density (left-hand panel) and the mass (right-hand panel) profiles of a representative model, after the baryon mass loss. The chosen run corresponds to the case ABA with instantaneous mass loss $\Delta t = 0$ Gyr and $\epsilon = 0.2$. The figure shows that the profile remains stable after $\sim$0.2 Gyr. The new equilibrium is reached within 40 dynamical times of the central region (equation 9). This holds true for all the other simulated cases.

A commonly made approximation in evaluating the effect of baryon expulsion (or condensation) on the DMH is to treat the baryonic component as a potential that changes in intensity without any variation in shape. Fig. 5 illustrates that this approximation leads to some underestimate of the slope flattening and of its (weak) dependence on the expulsion time-scale. This is due to the fact that the mass loss actually causes a significant broadening of the baryon concentration in the centre, which changes the shape of the potential and is more important for shorter time-scales (Paper I). Therefore, in the full computation, the DM distribution is flattened not only by the decrease of gravitational force of baryons, but also by the (time-scale-dependent) outside dragging, due to the expansion of the leftover baryonic matter.

4 DISCUSSION AND CONCLUSIONS

A well-known general prediction of cosmological, gravity-only, simulations is that DMHs should have cuspy density profiles, essentially independently of the mass scale.[1] Observations at small to medium galactic scales (dwarf galaxies, disc-dominated LSB galaxies, as well as normal spirals) have demonstrated that this is not the case. At cluster scales, where DM is gravitationally subdominant in the central region, the situation is instead far from clear, with several claims for cored (e.g. Richtler et al. 2011) as well as for cuspy (e.g. Zitrin et al. 2011) density profiles. The former mismatch is widely ascribed to the back reaction of baryons, whose evolution to form galaxies is driven by various non-gravitational processes, on DM particles. The intermediate regime of large ETGs, the subject of our work, has received so far much less attention, both from the observational and theoretical points of view. As for the former, again there are interpretations favouring a cored (e.g. Memola et al. 2011) as well as a cuspy (Tortora et al. 2010; Sonnenfeld et al. 2011) density profile. Firm conclusions are, however, severely plagued by the degeneracy between the initial mass function and the DM density profiles (Treu et al. 2010).

In this paper, we have elucidated that an important gas removal during the early evolution of ETGs should leave as a by-product sizeable signatures also on the inner profile of their DMHs. A similar ejection is required by most galaxy formation models aiming to explain the basic properties of these systems, such as their chemical properties, low baryon content or luminosity function (e.g. Benson et al. 2003; Granato et al. 2004; Pipino, Silk & Matteucci 2009; Duffy et al. 2010), and it is commonly, but not always, ascribed to *QSO mode* AGN feedback. The DM density profile ends up to be significantly less concentrated than NFW, unless the prior (opposite) contraction generated by baryon collapse and condensation has been very efficient, and probably unrealistic, i.e. closer to that estimated on the basis of approximate analytical treatments (e.g. Blumenthal et al. 1986) than to that found in most cosmological simulations (e.g. Abadi et al. 2010; Gnedin et al. 2011).

Moreover, it has been pointed out that stellar feedback can weaken the DM cusp in dwarf and spiral galaxies not only by means of gas removal from the galaxy potential well, but also as a consequence of oscillations of the potential generated by bulk motions of gas within the galaxy (Mashchenko et al. 2006, 2008; Macciò et al. 2012; Pontzen & Governato 2012). Similar fluctuations could be induced, for instance, by non-isotropic gas removal for the AGN feedback. Although, for simplicity and lack of theoretical understanding, models of galaxy formation treat AGN feedback by means of isotropic subgrid prescriptions, the case for preferential directions for the effect of AGN activity on its environment is actually strong. Indeed, all our knowledge of the AGN phenomenon points to a non-isotropic structure, including accretion discs, jets, ionization cones and dust tori. More specifically, recent observational evidence directly indicates non-isotropic quasar-driven gas removal (e.g. Cano-Diaz et al. 2012). To explore properly this effect would require more complex numerical experiments, possibly including a treatment of gas dynamics. The effort seems somewhat premature at present, given the lack of understanding of how AGN gas removal works, and we

[1] Note that this feature has also been found recently in self-similar analytic models for the halo collapse (e.g. Lapi & Cavaliere 2011).

leave it for future investigations.[2] In any case, it is worth noting that this possible additional process could even enhance the flattening effect of AGN feedback on the DM distribution estimated here.

Martizzi et al. (2012) suggested that several mechanisms contribute to the formation of the $\sim$10 kpc core in the brightest cluster galaxy of a simulated Virgo-like galaxy cluster ($M_{\rm vir} \simeq 10^{14}\,{\rm M}_{\odot}$) found when (and only when) subgrid models for the growth of supermassive black holes and the ensuing feedback are included in their hydrosimulation. Our idealized numerical experiments elucidate and quantify the important contribution of one of these mechanisms, namely the ejection of baryonic matter (representing gas).

In conclusion, cuspy density profiles in ETGs, tentatively inferred from some recent observation, could be difficult to reconcile with an effective AGN (or stellar) feedback, in particular that believed to cause massive galactic winds during the early evolution of these systems, making them *red and dead*.

ACKNOWLEDGMENTS

CR-F and GLG acknowledge the warm hospitality by INAF-Trieste and IATE-Córdoba, respectively, during the development of this work. We thank A. Lapi, P. Salucci, J. Navarro and A. Meza for several useful discussions on the topic of this work. This work has been partially supported by the Consejo de Investigaciones Científicas y Técnicas de la República Argentina (CONICET), the Secretaría de Ciencia y Técnica de la Universidad Nacional de Córdoba (SeCyT) and the European Commissions Framework Programme 7 through the International Research Staff Exchange Scheme LACEGAL.

REFERENCES

Abadi M. G., Navarro J. F., Fardal M., Babul A., Steinmetz M., 2010, MNRAS, 407, 435
Benson A. J., Pearce F. R., Frenk C. S., Baugh C. M., Jenkins A., 2001, MNRAS, 320, 261
Benson A. J., Bower R. G., Frenk C. S., Lacey C. G., Baugh C. M., Cole S., 2003, ApJ, 599, 38
Blumenthal G. R., Faber S. M., Flores R., Primack J. R., 1986, ApJ, 301, 27
Brammer G. B. et al., 2011, ApJ, 739, 24
Bryan G. L., Norman M. L., 1998, ApJ, 495, 80
Buote D. A., Humphrey P. J., 2012, in Kim D.-W., Pellegrini S., eds, Astrophysics Space Science Library Vol. 378, Hot Interstellar Matter in Elliptical Galaxies. Springer, Berlin, p. 235
Cano-Diaz M., Maiolino R., Marconi A., Netzer H., Shemmer O., Cresci G., 2012, A&A, 537, L8
Cattaneo A., Dekel A., Devriendt J., Guiderdoni B., Blaizot J., 2006, MNRAS, 370, 1651
Cattaneo A. et al., 2007, MNRAS, 377, 63
Ciotti L., Ostriker J. P., Proga D., 2009, ApJ, 699, 89
de Blok W. J. G., 2010, AdAst, 2010
de Souza R. S., Rodrigues L. F. S., Ishida E. E. O., Opher R., 2011, MNRAS, 415, 2969
Dubinski J., Carlberg R. G., 1991, ApJ, 378, 496
Duffy A. R., Schaye J., Kay S. T., Dalla Vecchia C., Battye R. A., Booth C. M., 2010, MNRAS, 405, 2161
Fabian A. C., 1999, MNRAS, 308, L39
Fontanot F., De Lucia G., Monaco P., Somerville R. S., Santini P., 2009, MNRAS, 397, 1776
Gnedin O. Y., Zhao H., 2002, MNRAS, 333, 299
Gnedin O. Y., Kravtsov A. V., Klypin A. A., Nagai D., 2004, ApJ, 616, 16
Gnedin O. Y., Ceverino D., Gnedin N. Y., Klypin A. A., Kravtsov A. V., Levine R., Nagai D., Yepes G., 2011, preprint(arXiv:1108.5736)
Governato F. et al., 2010, Nat, 463, 203
Granato G. L., Silva L., Monaco P., Panuzzo P., Salucci P., De Zotti G., Danese L., 2001, MNRAS, 324, 757
Granato G. L., De Zotti G., Silva L., Bressan A., Danese L., 2004, ApJ, 600, 580
Helly J. C., Cole S., Frenk C. S., Baugh C. M., Benson A., Lacey C., Pearce F. R., 2003, MNRAS, 338, 913
Hernquist L., 1990, ApJ, 356, 359
Inoue S., Saitoh T. R., 2011, MNRAS, 418, 2527
Johansson P. H., Naab T., Burkert A., 2009, ApJ, 690, 802
Kazantzidis S., Magorrian J., Moore B., 2004, ApJ, 601, 37
Klypin A., Trujillo-Gomez S., Primack J., 2011, ApJ, 740, 102
Komatsu E. et al., 2009, ApJS, 180, 330
Lapi A., Cavaliere A., 2011, ApJ, 743, 127
Macciò A. V., Stinson G., Brook C. B., Wadsley J., Couchman H. M. P., Shen S., Gibson B. K., Quinn T., 2012, ApJ, 744, L9
Martizzi D., Teyssier R., Moore B., Wentz T., 2012, MNRAS, 2773
Mashchenko S., Couchman H. M. P., Wadsley J., 2006, Nat, 442, 539
Mashchenko S., Wadsley J., Couchman H. M. P., 2008, Sci, 319, 174
Memola E., Salucci P., Babić A., 2011, A&A, 534, A50
Monaco P., Fontanot F., Taffoni G., 2007, MNRAS, 375, 1189
Moster B. P. et al., 2010, ApJ, 710, 903
Navarro J. F., Eke V. R., Frenk C. S., 1996, MNRAS, 283, L72
Navarro J. F., Frenk C. S., White S. D. M., 1997, ApJ, 490, 493
Newman A. B., Ellis R. S., Bundy K., Treu T., 2012, ApJ, 746, 162
Ogiya G., Mori M., 2011, ApJ, 736, L2
Pasetto S., Grebel E. K., Berczik P., Spurzem R., Dehnen W., 2010, A&A, 514, A47
Peirani S., Kay S., Silk J., 2008, A&A, 479, 123
Pipino A., Silk J., Matteucci F., 2009, MNRAS, 392, 475
Pontzen A., Governato F., 2012, MNRAS, 2641
Pooley D., Rappaport S., Blackburne J. A., Schechter P. L., Wambsganss J., 2012, ApJ, 744, 111
Ragone-Figueroa C., Granato G. L., 2011, MNRAS, 414, 3690 (Paper I)
Read J. I., Gilmore G., 2005, MNRAS, 356, 107
Richtler T., Salinas R., Misgeld I., Hilker M., Hau G. K. T., Romanowsky A. J., Schuberth Y., Spolaor M., 2011, A&A, 531, A119
Salucci P., Frigerio Martins C., 2009, EAS Publication Series Vol. 36, p. 133
Sijacki D., Springel V., Di Matteo T., Hernquist L., 2007, MNRAS, 380, 877
Silk J., Rees M. J., 1998, A&A, 331, L1
Somerville R. S., Hopkins P. F., Cox T. J., Robertson B. E., Hernquist L., 2008, MNRAS, 391, 481
Sonnenfeld A., Treu T., Gavazzi R., Marshall P. J., Auger M. W., Suyu S. H., Koopmans L. V. E., Bolton A. S., 2011, preprint (arXiv:1111.4215)
Springel V., 2005, MNRAS, 364, 1105
Tonini C., Lapi A., Salucci P., 2006, ApJ, 649, 591
Tortora C., La Barbera F., Napolitano N. R., de Carvalho R. R., Romanowsky A. J., 2012, preprint (arXiv:1201.2945)
Treu T., Auger M. W., Koopmans L. V. E., Gavazzi R., Marshall P. J., Bolton A. S., 2010, ApJ, 709, 1195
Viola M., Monaco P., Borgani S., Murante G., Tornatore L., 2008, MNRAS, 383, 777
Zhao D. H., Mo H. J., Jing Y. P., Börner G., 2003, MNRAS, 339, 12
Zitrin A. et al., 2011, ApJ, 742, 117

[2] Peirani et al. (2008) performed idealized numerical experiments partly in this spirit, in which periodic AGN activity is assumed to cause bulk oscillations, rather than removal, of gas. See also discussion in Potzen & Governato (2012).

This paper has been typeset from a TEX/LATEX file prepared by the author.